

Cyclic voltammetric behavior of iron electrode in sodium hydroxide solutions

I. ZAAFARANY

Department of Chemistry, Faculty of Applied Science, Umm Al-Qura University,
P.O. Box 118, Makkah Al Mukaramha (Saudia Arabia).

(Received: March 10, 2009; Accepted: May 15, 2009)

ABSTRACT

The electrochemical behaviour of iron electrode in different concentrations and sweep rate of NaOH solution were studied using cyclic voltammograms. Four anodic peaks (A_1 - A_4) were observed in the anodic scan of cyclic voltammograms where as two cathodic peaks (C_1 and C_2) were observed in the cathodic scan of cyclic voltammograms. The four anodic peaks due to the formation $Fe(OH)_{ads}$ peak (A_1), $Fe(OH)_2$ peak (A_2), Fe_2O_3 (peak A_3) and formation of more stable $Fe(III)$ species (peak A_4) and the cathodic scan due to the reduction of species formed on the anodic scan.

Key words: Iron electrode, NaOH, Cyclic voltammograms, Electrochemistry.

INTRODUCTION

Iron is one of the metal used in several fields of industry. Iron and similar metals are exposed to corrosion in connection with environmental conditions. The corrosion rate varies subject to structure of ions and molecules, kind and concentration of ions, nature of solution and type of materials^{1,2}.

Oxidation and reduction process taking place on iron electrode in alkaline media are important from the point of view of alkaline accumulators, and many authors³⁻⁵ have dealt with the reaction mechanism and influence of additives, etc.

Extensive studies of the iron electrodes in alkaline solution have been presented in numerous publications⁶⁻⁹. Two main reasons of this great

interest can be given: On one hand, iron electrodes in alkaline solution could be appropriate for various accumulator applications (Fe /NiOOH, Fe/air etc). On the other hand, iron is one of the most important metal in modern technology. Corrosion problems cover the whole range of pH in aqueous systems from acidic to basic, solutions.

Iron electrodes for batteries are normally placed in concentrated alkali solution 5M KOH. The charged state of the battery in Fe (O) gained by electrochemical reduction (discharge). The discharge reaction first leads to Fe(II), which is found to be $Fe(OH)_2$ ¹⁰. Prolonged discharge leads to the formation of a sludge which was identified by in situ Mössbauer spectroscopy during cyclic galvanostatic oxidation-reduction of iron and found to be mainly $Fe(OOH)$ and unreacted $Fe(OH)_2$ ¹¹ on numerous occasions, it has been pointed out that the formation of oxides involves soluble Fe(II) and Fe(III) species¹².

EXPERIMENTAL

Methods

The test electrode was made up of pure Iron obtained from Saudi iron and steel Company and having the following chemical composition (wt%) (C,0.052, Mn 0.189, S0.011, P 0.008, Si 0.011, Al 0.039, N 0.001, Cr 0.012, Cu 0.04, Mo 0.024, Ni 0.029, and the remaining is iron). A cylindrical iron rod embedded in aralidite with exposed surface area of 0.5 cm². Prior to each experiment, the surface of iron specimen were mechanically polished with different grades of emery paper, degreased with acetone and rinsed in distilled water. No attempts were made to deareate them. The electrolytic cell was all Pyrex and described elsewhere¹³.

Cyclic voltammograms curves (CVs) were performed using auto lab (ECO Chemie) combined with the software package GPES (General Purpose

Electrochemical System). This is a computer controlled electrochemical measurement system. It consists of data acquisition system and potentiostat-galvanostat. CV's were used to study the electrochemical behaviour of iron in different concentrations of NaOH solutions sweeping from hydrogen evolution to oxygen evaluation. All measurements were taken at 25 ± 1°C.

RESULTS AND DISCUSSION

Cyclic voltammogram behavior of iron electrode in NaOH solutions

The concentration range investigated was 0.1-5M NaOH (PH=13-14). Typical voltammograms are shown in Figs. 1 to 3. All the curves correspond to multicycling. The obtained voltammograms are similar to that published by Burke and Lyons¹⁴, who used solutions of NaOH as the electrolyte. At a concentration of 1M NaOH, four anodic peaks (A₁ – A₄) and two cathodic peaks (C₁ and C₂) were

Table 1: The charge density and film thickness results from the cyclic voltammograms of an iron electrode in 1M NaOH

Sweep rate(mV/s)	Total anodic charge density (Q _a) (C/cm ²)	Peak height (I _p) A ₃	Peak Potential (E _p) A ₃	Charge density of A ₃ (C/cm ²)	Film thickness(nm)
1	1.858e-3	1.24e-5	-0.747	5.813e-4	10.35
5	2.102e-3	1.471e-5	-0.702	7.631e-4	10.01
10	2.606e-3	2.942e-5	-0.672	9.618e-4	9.14
30	2.434e-3	6.919e-5	-0.628	9.691e-4	8.54
50	3.268e-3	0.932e-3	-0.623	6.505e-3	7.93
100	4.536e-3	1.863e-3	-0.612	7.318e-3	4.2
150	5.891e-3	2.768e-3	-0.608	9.656e-3	4.06

Table 2: The multicycles effect on the film of an iron electrode in 1M NaOH

Number of cycles	Total anodic charge density (Q _a) (C/cm ²)	Peak height (I _p) A ₃	Peak Potential (E _p) A ₃	Charge density of A ₃ (C/cm ²)
1	4.536e-3	1.201e-3	-0.620	3.286e-3
2	4.289e-3	1.225e-3	-0.618	3.414e-3
3	4.273e-3	1.244e-3	-0.616	3.521e-3
4	4.295e-3	1.261e-3	-0.614	3.610e-3
5	4.326e-3	1.275e-3	-0.614	3.682e-3
6	4.360e-3	1.288e-3	-0.612	3.738e-3
7	4.394e-3	1.300e-3	-0.612	3.781e-3

observed; at lower concentrations, the peaks A_2 and A_4 decrease. The current of peaks A_3 and C_2 increase with the number of cycles; their dependence on the $NaOH$ concentration passes through a maximum in the region 1M, corresponding

to the maximum charge delivered by the electrode during one cycle. By a suitable choice of the limiting anodic potential it can be shown that the peak C_2 is related to A_3 and the peak C_1 is related to both A_1 and A_2 , *Fig. 1*. Thus, the couple C_2 - A_3 belongs to

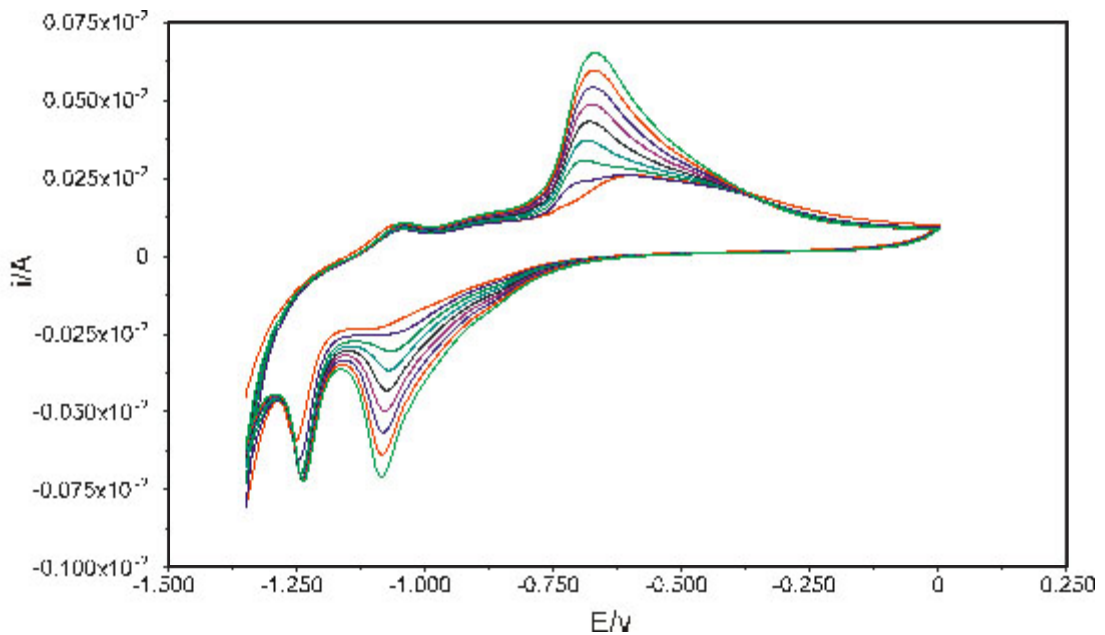


Fig. 1: Cyclic Voltammetry of iron in 2M $NaOH$ at sweep rate 1mV/s, (SCE)

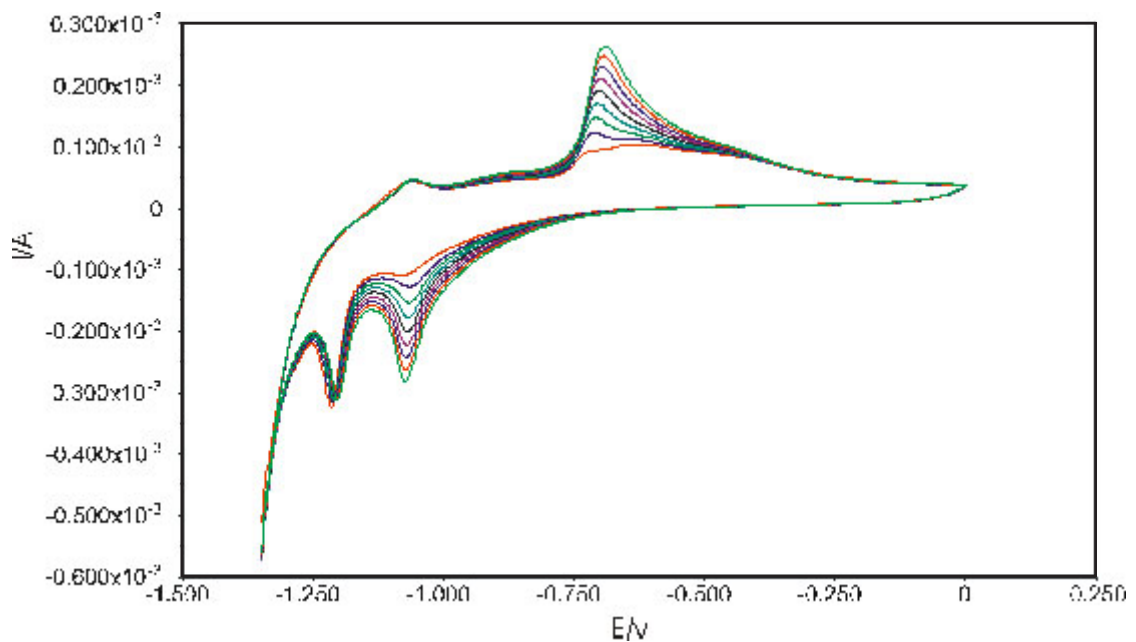


Fig. 2: Cyclic Voltammetry of iron in 0.1M $NaOH$ at sweep rate 30mV/s, (SCE)

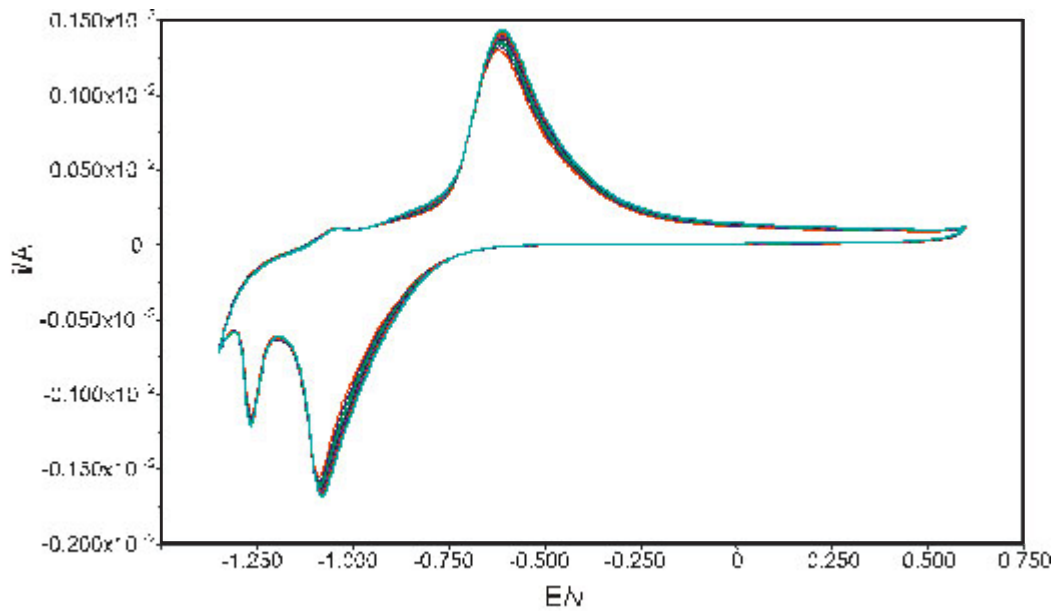


Fig. 3: Cyclic Voltammetry of iron in 5M NaOH at sweep rate 100mV/s, (SCE)

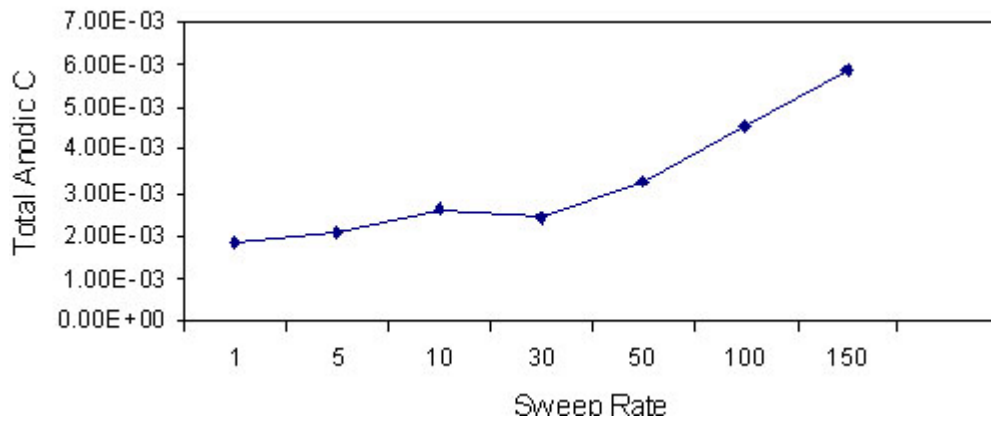


Fig. 4: Effect of the sweep rate on the total anodic charge density for iron electrode in 1M NaOH

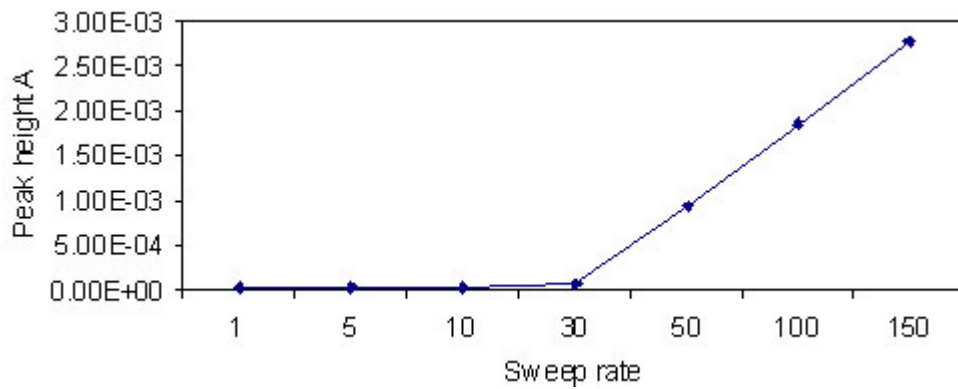


Fig. 5: Effect of the sweep rate on the peak height of A³ for for iron electrode in 1MNaOH

one redox system and the triad C_1 - A_1 , A_2 to another, couple.

Fundamentally similar behaviors in 0.1M NaOH solution were also obtained for 1M NaOH solution, *Fig. 1- 3* but it was recognized from these results that especially, peak A_3 and peak C_2 decreased in accordance with increase in the

concentration of NaOH whereas peak C_1 increased in a region of high concentration of NaOH. A well defined anodic peak A_5 in the transpassive region and cathodic peak C_3 conjugated to peak A_5 , *Fig. 1* were observed in 2M NaOH solutions. The low concentration of OH^- ions, resulting in a low O_2 evolution current, ($E^\ominus = 1.23 - 0.059 \text{ PH}$) allowed the anodic limit to be increased.

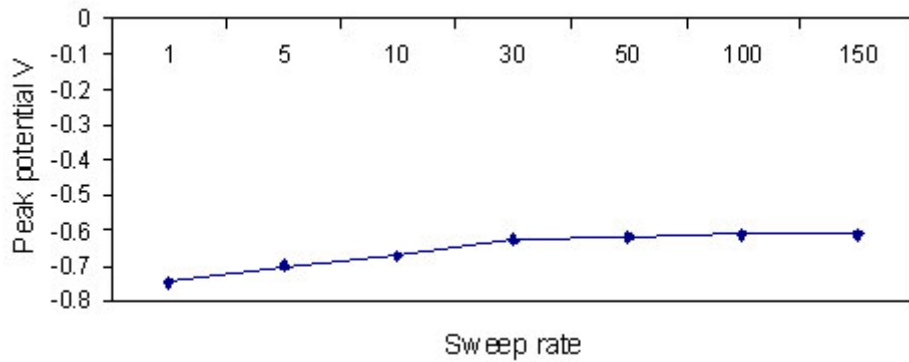


Fig. 6: Effect of the sweep rate on the peak potential A^3 for iron electrode in 1MNaOH

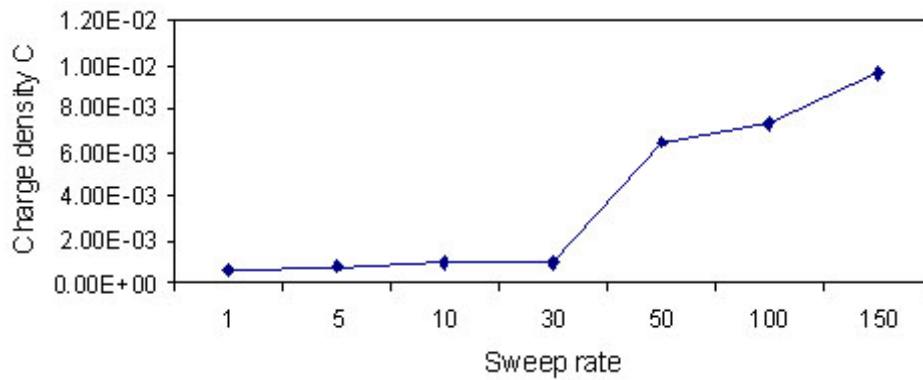


Fig. 7: Effect of the sweep rate on the charge density A^3 for iron electrode in 1MNaOH

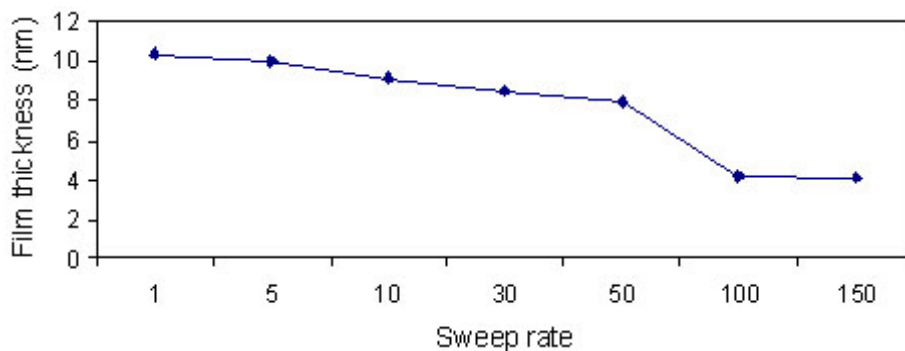


Fig. 8: Effect of the sweep rate on the Film thickness for iron electrode in 1MNaOH

The general shape of the cyclic voltammograms, however, was similar to that obtained in 2M NaOH, suggesting that the composition of the film, both in the passive and in the active region is the same in hydroxide. The peak

A_0 at the upper end of the potential corresponds to the oxygen gas evolution reaction and the peak C_0 at lower end of the potential corresponds to hydrogen gas evolution reaction Fig.1. With increasing sweep rate, the peak potential of A_2 and

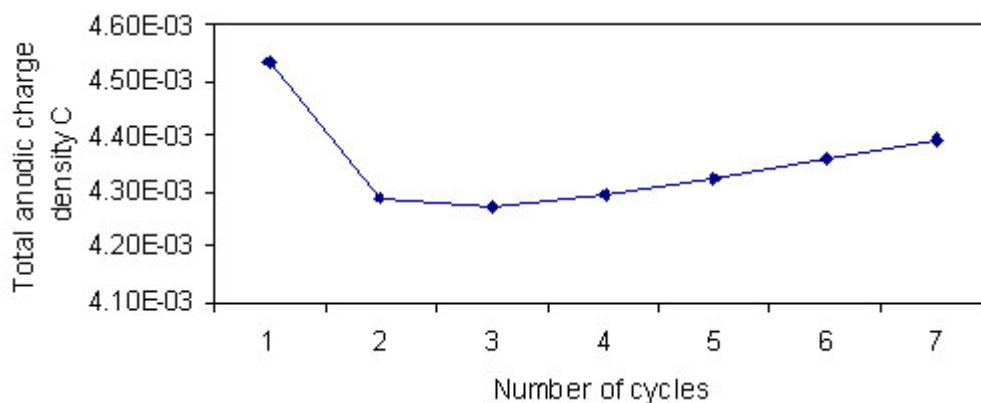


Fig. 9: Effect of the multi cycles on the total anodic charge density (Q_a) (C/cm^2) for iron electrode in 1MNaOH

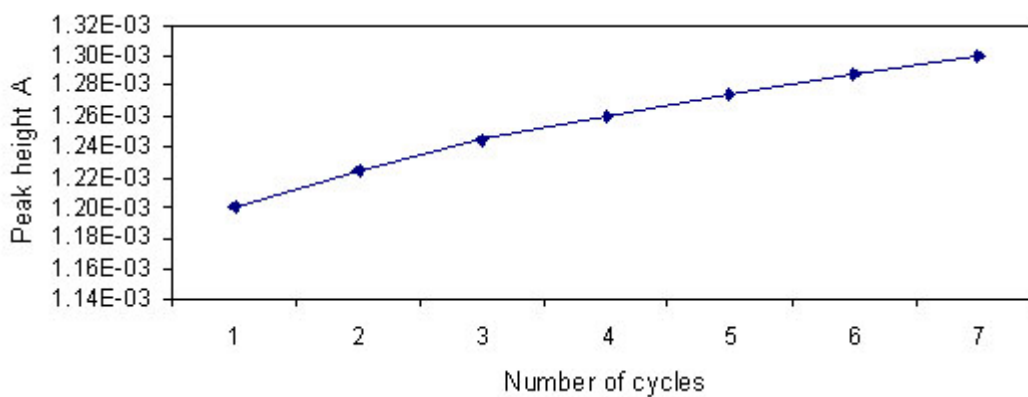


Fig. 10 : Effect of the multi cycles on the peak height A^3 for iron electrode in 1MNaOH

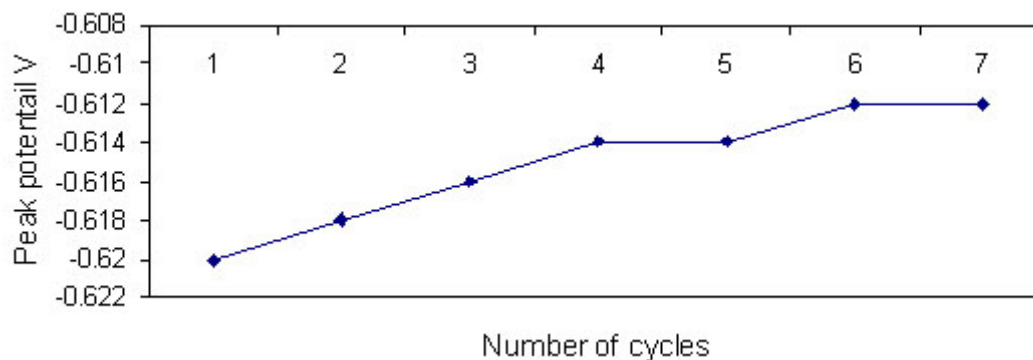


Fig. 11 : Effect of the multi cycles on the peak potential A^3 for iron electrode in 1MNaOH

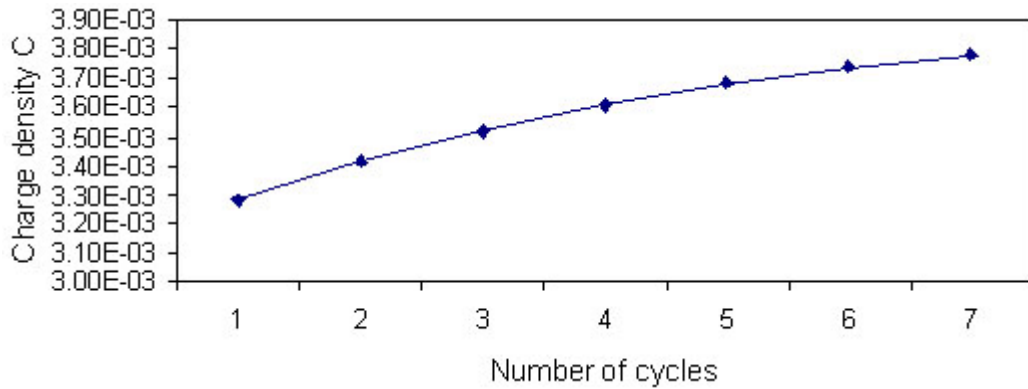


Fig. 12 : Effect of the multi cycles on the charge density A^3 for iron electrode in 1MNaOH

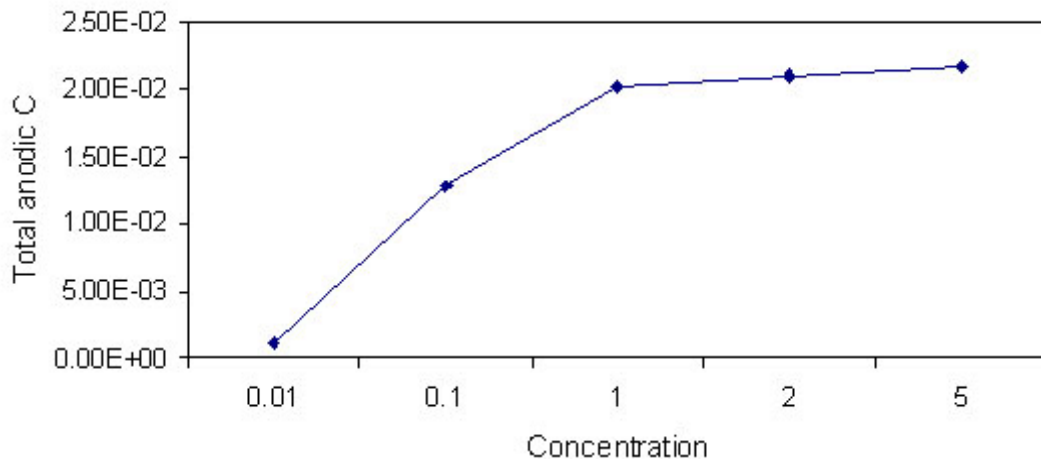


Fig. 13 : Effect of the concentration on the total anodic charge density for iron electrode in NaOH solutions

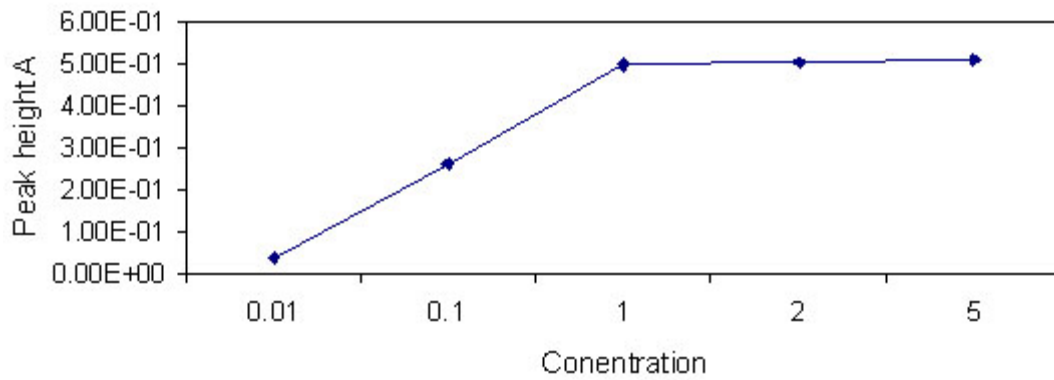


Fig. 14 : Effect of the concentration on the peak height A^3 for iro electrode in NaOH solutions

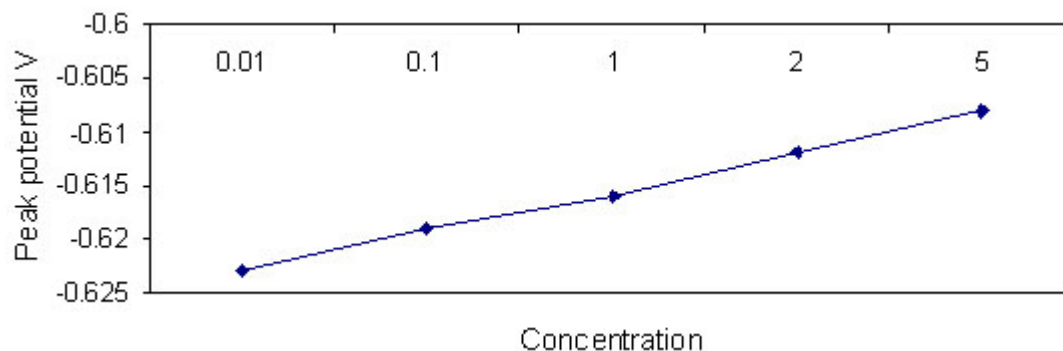


Fig. 15 : Effect of the concentration on the peak potential A_3 for iron electrode in NaOH solutions

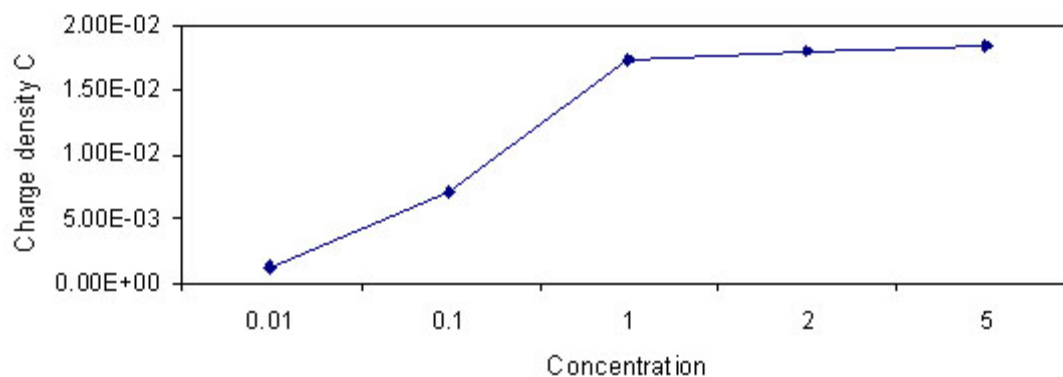


Fig. 16: Effect of the concentration on the charge density A_3 for iron electrode in NaOH solutions

A_3 are shifted to more positive values, whereas those of the C_1 and C_2 are shifted in the negative direction. The best curve shape was obtained at sweep rate 40-50 mVs⁻¹. The positions of the peaks on the potential scale, their relative orders of magnitude, and their behavior during cycling as observed are shown in Fig.1 to 3. There is general agreement that the voltammograms of iron in strongly alkaline media involve two conspicuous

peaks, an anodic and a cathodic one (A_3 and C_2) their current increase with increasing number of cycles up to a limit. Their potentials vary appreciably (anodic from -0.67 to -0.40V, cathodic from -1.15 to -0.85V). The reasons why the peak potentials vary are not always clear. The peaks A_3 and C_2 , Fig.1, appear relatively small on the first cycle, but they increase with number of cycles, evidence for thickening of the formed oxide film.

Table 3: The concentration effect on the film of an iron electrode in NaOH

Concentration	pH	Total anodic charge density (Q_a) (C/cm ²)	Peak height (I_p) A_3	Peak Potential (E_p) A_3	Charge density of A_3 (C/cm ²)
0.01	12	1.23e-3	38e-3	-0.623	1.236e-3
0.1	13	12.805 e-3	260e-3	-0.619	7.125e-3
1	14	20.161 e-3	500e-3	-0.616	17.354e-3
2	14	20.919 e-3	505e-3	-0.612	17.996e-3
5	14	21.677 e-3	510e-3	-0.608	18.524e-3

Influence of sweep rate and concentration

It was demonstrated previously that two of the most important factors influencing the development of charge storage capacity in the case of iron electrodes were the values for the upper and lower limit of the potential sweep. The observed optimum values 1.4V for the lower limit and + 0.6V for the upper limit, were adopted throughout the present investigation. A relatively small number of oxide growth cycles were used in most experiments in order to maintain reasonably small current values (and hence, minimize potential errors associated with iR drop) and to ensure a high level of reactivity throughout the surface layer. Figs. 4-8 show the influences of the sweep rate on the CVs. The CV for sweep rate 1mv/s shows rather complicated features that are beginning to be smeared out at 10mv/s. This shows that the kinetics of the electrode processes are rather slow. At lower sweep rates the layers formed are thicker than at higher sweep rates. In Figs. 13-16. the influence of the concentration on the CV is shown.

Development of charge capacity

Charge measurements were performed on the voltammograms by two methods, the first one by using computer integration for the relevant area of interest (peak A_3), and the second by photocopying the results, cutting out the relevant area and weighing it relative to an area of known dimensions.

The charge was calculated as being the area/sweep rate and subsequent division by the area of the electrode (0.1964cm^2) gives the charge density, Q . The charges obtained by the two methods were quite similar; for peak $A_3 = 6.02 \pm 0.5$ mC/cm^2 by weighing and 7 ± 0.5 mC/cm^2 , by

computer integration. The total anodic charge density 14.626 mC/cm^2 is larger than the cathodic charge density 10.632 $\text{mC/cm}^2 \pm 0.53$ (was found to be about 25%). The influence of different factors on the charge density, peak height and film thickness are presented in *Tables 1 to 3*.

Under multicycle conditions the charge density and the film thickness increase with cycle number as shown in Figs. 9-12. The film is reported to be more stable at room temperature and in concentrated alkaline solution, Figs. 13-16.

The dependence of peak height on sweep rate appears to be linear, Fig. 7. A detail analysis of the sweep rate dependence would require more measurements over a wider range of sweep rate. At low sweep rates it is likely that there is dissolution occurs in the Fe^{2+} region i.e. $\text{Fe}(\text{OH})_2$ is soluble to a certain extent then the thickness is overestimated. The film thickness is about 4nm, Fig. 8, which agree with other methods like ellipsometry.

A marked dependence of charge capacity development on the oxide growth sweep rate was calculated from Figs. 4-8. The nature of this dependence is influenced by the layer thickness, which is usually decreasing of higher sweep rates. Fig. 8, and Table 1 show that Q_A decreases with the increase of the sweep rate and finally is attaining a constant value.

The variation of charge capacity development with increasing number of oxide growth cycles are outlined in Figs. 9-12, and Table 2. The anodic charge, Q_A , consumed in the potential range $1.4\text{V} \leq E \leq 0.6\text{V}$. Q_A increase almost linearly with oxide thickness and pH (Figs. 13-16 Table 3)

REFERENCES

1. S. Zor, B. Yazici and M. Erbil: *Corros. Sci.*, **47**: 2700 (2005).
2. S. Zor. Turkish: *J. Chem.* **26**: 403 (2002).
3. J. Cerny and K. Micka: *J. of Power Sources* **25**: 111 (1989).
4. L. Ojefors: *J. Electrochem. Soc.* **123**: 1691 (1976).
5. E.B. Castro: *Electrochim. Acta*, **14**: 2117 (1994).
6. A. El-Sayed: *Revue Roumaine de chimie*: **38**(2): 139 (1993).

7. B. Anderson and L. Ojefors: *J. Electrochem. Soc.* **123**: 814 (1976).
8. D.D. Macdonald and D.Owen: *J. Electrochem. Soc.*, **120**: 317(1973).
9. F. Beck, R. Kaus and M. Oberst: *Electrochim Acta* **30**(2): 173 (1985).
10. H.G. Silver and E. Leaks: *J. Electrochem. Soc.*, **117**: 5 (1970).
11. Y. Geronov, I. Tonov and S. Georgiev: *J. Appl. Electrochem.*, **5**: 351 (1974).
12. T. Hurlen, *Electrochim. Acta*, **8**: 609 (1963).
13. A. M. Shams El-Din and S.M. Abd El-Haleem, *Werkst. Korros.*, **24**: 389 (1973).
14. Z.D. Burke and M.E.G. Lyons: *J. Electroanal. Chem.* **198**: 347 (1986).